Diffusive epidemic process: theory and simulation

2007 J. Phys.: Condens. Matter 19 065143

(http://iopscience.iop.org/0953-8984/19/6/065143)

INSTITUTE OF PHYSICS PUBLISHING JOURNAL OF PHYSICS: CONDENSED MATTER

J. Phys.: Condens. Matter **19** (2007) 065143 (16pp) doi:10.1088/0953-8984/19/6/065143

Diffusive epidemic process: theory and simulation

Daniel Souza Maia and Ronald Dickman

Departamento de Física, Instituto de Ciências Exatas, Universidade Federal de Minas Gerais, CP 702, 30123-970, Belo Horizonte, Minas Gerais, Brazil

E-mail: dfmaia@ufmg.br and dickman@fisica.ufmg.br

Received 31 July 2006, in final form 7 November 2006
Published 22 January 2007
Online at stacks.iop.org/JPhysCM/19/065143

Abstract

We study the continuous absorbing-state phase transition in the one-dimensional diffusive epidemic process via mean-field theory and Monte Carlo simulation. In this model, particles of two species (A and B) hop on a lattice and undergo reactions $B \to A$ and $A + B \to 2B$; the total particle number is conserved. We formulate the model as a continuous-time Markov process described by a master equation. A phase transition between the (absorbing) B-free state and an active state is observed as the parameters (reaction and diffusion rates, and total particle density) are varied. Mean-field theory reveals a surprising, nonmonotonic dependence of the critical recovery rate on the diffusion rate of B particles. A computational realization of the process that is faithful to the transition rates defining the model is devised, allowing for direct comparison with theory. Using the quasi-stationary simulation method we determine the order parameter and the survival time in systems of up to 4000 sites. Due to strong finite-size effects, the results converge only for large system sizes. We find no evidence for a discontinuous transition. Our results are consistent with the existence of three distinct universality classes, depending on whether A particles diffusive more rapidly, less rapidly or at the same rate as B particles. We also perform quasi-stationary simulations of the triplet creation model, which yield results consistent with a discontinuous transition at high diffusion rates.

(Some figures in this article are in colour only in the electronic version)

1. Introduction

This work is devoted to the one-dimensional diffusive epidemic process (DEP) [1], a model system in which two kinds of particles, A and B, diffuse on a lattice and undergo reactions $B \to A$ and $A + B \to 2B$. There is no intrinsic limit on the number of particles that may

be present at a given site; the total number of particles is conserved. In the epidemic interpretation A represents a healthy organism and B an infected one, with the reactions above corresponding, respectively, to spontaneous recovery and transmission of disease on contact. Other interpretations are possible, for example, A could represent a properly folded protein and B a misfolded one, etc.

The DEP is a nonequilibrium stochastic model exhibiting a phase transition to an absorbing state [2–5]. Such phase transitions arise in many models of epidemics, population dynamics and autocatalytic chemical reactions, and have attracted much interest in nonequilibrium statistical mechanics, in efforts to characterize the associated universality classes. The simplest example is the contact process (CP), or its discrete-time version, directed percolation (DP). In the CP, each site of a lattice is either vacant (0) or occupied by a particle (X). Particles die (i.e. the reaction $\mathrm{X} \to 0$) at rate 1, independent of the configuration of the rest of the system, and reproduce at rate λ (reaction $\mathrm{X} + 0 \to 2\mathrm{X}$). The offspring particle survives if and only if the site it is sent to (selected at random from the neighbours of the reproducing particle) is vacant. The CP is therefore a minimal model for birth-and-death processes with local competition for space. The particle-free configuration is absorbing. It is known that for reproduction rate $\lambda < \lambda_c$ the stationary density of particles ρ is zero, and that (in the infinite system size limit) ρ grows continuously from zero as λ is increased beyond λ_c. Thus ρ serves as the order parameter for this phase transition.

Critical scaling in the contact process and allied models has been studied extensively, both theoretically and numerically. A central conclusion deriving from these studies is that critical behaviour of the DP type is generic for models exhibiting a continuous phase transition to an absorbing state, in the absence of any additional symmetries or conserved quantities. (Note that the absorbing state may in some cases encompass more that one configuration, as is the case in the pair contact process [6]. If these configurations are not related by any symmetry the critical behaviour is still expected to fall in the DP universality class.) Particularly relevant in the present context is the fact that the *diffusive* CP (in which particles hop at a finite rate) also belongs to the DP class [7].

The DEP offers a more complicated scenario of scaling. Let D_A (D_B) denote the diffusion rate of A (B) particles. An especially interesting aspect of the DEP is that the absorbing-state phase transition appears to belong to three distinct classes, depending on whether $D_\mathrm{A} < D_\mathrm{B}$, $D_\mathrm{A} = D_\mathrm{B}$ or $D_\mathrm{A} > D_\mathrm{B}$. The renormalization group (RG) analysis of Oerding *et al* [8] predicts a continuous phase transition in the first two cases. But for $D_\mathrm{A} > D_\mathrm{B}$ the RG analysis yields a discontinuous transition. These authors provide numerical evidence of such a transition in two dimensions; numerical studies of the one-dimensional DEP, however, show a continuous phase transition [9].

The diffusive epidemic process was initially studied via RG methods [1, 8, 10]. Numerical simulations for equal diffusion rates were reported in [11], yielding results in disagreement with the RG prediction $\nu_\perp = 2$ (see [12, 13]). Subsequently, the simulations reported in [9] appeared to resolve this point, but suggested other departures from RG predictions in the one-dimensional case.

Given the disagreement between theory and simulation, it is of interest to perform further analysis of the DEP. In the present work we study a one-dimensional version of the process, formulated in continuous time, in a manner allowing for a simple formulation of the master equation. We study this process (defined in detail in the following section), using one- and two-site mean-field theory (section 3), and Monte Carlo simulation (section 4) using the quasi-stationary simulation method. The functioning of the simulation method at a discontinuous phase transition is examined in section 5 by applying it to the triplet creation model. Conclusions and open questions are discussed in section 6.

2. Model

The DEP is defined on a lattice of L^d sites. A configuration is specified by the set of variables a_j and b_j, denoting the number of A and B particles at each site j. There are no intrinsic restrictions on the number of particles at each site, making this process, in the language commonly employed in the literature, a 'bosonic' model. (To avoid confusion we note that quantum statistics do not enter into the problem.) The model is a continuous-time Markov process characterized by four kinds of transition:

- Hopping of A particles to a randomly chosen nearest neighbour (NN) site, at rate D_A.
- Hopping of B particles to a randomly chosen NN site, at rate D_B.
- Transformation of B particles to A particles, at rate r.
- Transformation of A particles to B particles, in the presence of a B particle at the same site, at a rate of λ per A–B pair.

This means that a given site j loses (via diffusion) an A particle at rate $D_A a_j$ (similarly for loss of a B particle), undergoes the process $B \to A$ at rate $r b_j$, and the process $A + B \to 2B$ at rate $\lambda a_j b_j$. Note that all transitions conserve the total particle number $N = \sum_j (a_j + b_j)$.

The process involves a rather large set of parameters: D_A, D_B, r, λ and the particle density $\rho = N/L^d$. Since one of the rates may be eliminated through a suitable scaling of time, we set $\lambda = 1$ from here on. This still leaves four control parameters. In the studies described below, we fix the diffusion constants and study the behaviour in the r–ρ plane, or fix D_A and ρ and treat D_B and r as the control parameters.

3. Mean-field theory

We begin by studying the model using dynamic mean-field theory (MFT) [2]. As is usual in cluster mean-field approaches, we assume spatial homogeneity from the outset, and then study the stationary solution of the equations of motion governing the probability distribution. In [8], using a continuum representation of the process, the mean-field limit is taken in the correct order (i.e. first $t \to \infty$, followed by the spatially uniform limit). The two approaches lead to qualitatively similar conclusions, i.e. a continuous phase transition. Here, by using the discrete-space formulation of the model, we are able to make specific numerical predictions for the transition point and the probability distribution. We present results for the one- and two-site approximations in one dimension, which follow from the master equation for the probability distribution $P(a_1, b_1; \ldots; a_L, b_L, t)$. Consider the evolution of the one-site marginal distribution $P(a, b)$:

$$\begin{aligned}
\dot{P}(a,b) = {} & D_A[(a+1)P(a+1,b) - aP(a,b)] \\
& + D_A \sum_{a',b'} a'[P(a-1,b;a',b') - P(a,b;a',b')] \\
& + D_B[(b+1)P(a,b+1) - bP(a,b)] \\
& + D_B \sum_{a',b'} b'[P(a,b-1;a',b') - P(a,b;a',b')] \\
& + r[(b+1)P(a-1,b+1) - bP(a,b)] \\
& + (b-1)(a+1)P(a+1,b-1) - abP(a,b). \qquad (1)
\end{aligned}$$

Here $P(a, b; a', b')$ is the joint probability distribution for a pair of NN sites. Equation (1) is the first in a hierarchy of equations for the probability distributions of $1, 2, \ldots, n, \ldots$ sites. At each level of the hierarchy, the diffusion terms couple the n-site distribution to that for

$n + 1$ sites. One-site MFT truncates this hierarchy at lowest order, via the factorization $P(a, b; a', b') = P(a, b)P(a', b')$, leading to,

$$\begin{aligned}\dot{P}(a,b) = {} & D_{\mathrm{A}}[(a+1)P(a+1,b) - aP(a,b)] + D_{\mathrm{A}}\rho_{\mathrm{A}}[P(a-1,b) - P(a,b)] \\ & + D_{\mathrm{B}}[(b+1)P(a,b+1) - bP(a,b)] + D_{\mathrm{B}}\rho_{\mathrm{B}}[P(a,b-1) - P(a,b)] \\ & + r[(b+1)P(a-1,b+1) - bP(a,b)] \\ & + (a+1)(b-1)P(a+1,b-1) - abP(a,b) \end{aligned} \tag{2}$$

where $\rho_{\mathrm{A}} = \sum_{a,b} aP(a, b)$ is the density of A particles and similarly for ρ_{B}. An equation for ρ_{A} is found by multiplying the above equation by a and summing over all values of a and b, giving

$$\dot{\rho}_{\mathrm{A}} = r\rho_{\mathrm{B}} - \langle ab \rangle \tag{3}$$

where $\langle a^m b^n \rangle \equiv \sum_{a,b} a^m b^n P(a, b)$. (Thus $\langle a \rangle = \rho_{\mathrm{A}}$ and similarly for ρ_{B}.) Note that, as discussed in detail below, the cross-moment $\langle ab \rangle$ is in general different from the simple product of A and B particle densities. If we nevertheless set $\langle ab \rangle = \rho_{\mathrm{A}}\rho_{\mathrm{B}}$, we have

$$\dot{\rho}_{\mathrm{A}} = r\rho_{\mathrm{B}} - \rho_{\mathrm{A}}\rho_{\mathrm{B}}. \tag{4}$$

With the constraint $\rho_{\mathrm{A}} + \rho_{\mathrm{B}} = \rho$, constant, we then find

$$\dot{\rho}_{\mathrm{B}} = (\rho - r)\rho_{\mathrm{B}} - \rho_{\mathrm{B}}^2 \tag{5}$$

showing that at this (lowest) level of approximation the order parameter ρ_{B} satisfies the Malthus–Verhulst equation with reproduction rate $\rho - r$. At this level, which may be called a 'rate equation', a continuous phase transition occurs at $\rho = r$, independent of the diffusion rates; the stationary density of B particles follows $\overline{\rho}_{\mathrm{B}} = \rho - r$. While the more detailed mean-field approximations described below yield a more reliable prediction for the phase boundary, we observe, in all cases, a continuous phase transition, and a linear relation between $\overline{\rho}_{\mathrm{B}}$ and $\rho - r_{\mathrm{c}}$ in the vicinity of the critical point (i.e. the usual mean-field critical exponent $\beta = 1$). We find no hint of a discontinuous transition.

A somewhat better result is obtained integrating (numerically) the full set of one-site MF equations, equation (2). In numerical analysis, it is necessary to truncate this set of equations at cutoff values a_{c} and b_{c}. This is justified since the probability distribution falls off exponentially for large a and/or b. The cutoff leads to certain technical restrictions in the numerical analysis. Naturally, transitions of the form $a_{\mathrm{c}} \to a_{\mathrm{c}} + 1$ must be excluded from consideration. Moreover, a transition of the form $a \to a - 1$, due to an A particle hopping away from the site of interest, must have its rate multiplied by $1 - P_{\mathrm{A}}(a_{\mathrm{c}})$, where $P_{\mathrm{A}}(a) = \sum_b P(a, b)$ is the one-site marginal distribution for the number of A particles. (Similar restrictions apply to transitions involving B particles.)

Once we take the full one-site probability distribution into account, the results for the phase boundary $\rho_{\mathrm{c}}(r)$ depend on the diffusion rates. Two factors enter into this dependence. First, in the vicinity of the phase transition, the reaction terms cause the marginal distribution for the number of B particles to deviate significantly from a Poisson distribution, while rapid diffusion tends to make the distribution more Poisson-like. Second, the reactions cause the variables a and b to be anti-correlated (that is, $\mathrm{cov}(a, b) = \langle ab \rangle - \rho_{\mathrm{A}}\rho_{\mathrm{B}} < 0$), whereas rapid diffusion tends to eliminate this correlation.

Figure 1 shows the critical line $\rho_{\mathrm{c}}(r)$ as predicted by the one-site MFT for various combinations of D_{A} and D_{B}. The higher the diffusion rates, the more closely ρ_{c} approaches the simple rate equation result $\rho_{\mathrm{c}} = r$. For finite diffusion rates ρ_{c} is always greater than r, due again to the anti-correlation of a and b. The critical value ρ_{c} appears to be more sensitive to D_{B} than D_{A}. In fact, for $D_{\mathrm{B}} = 0.2$, the curves for $D_{\mathrm{A}} = 0.2$ and 1 are virtually identical. (For larger values of D_{B}, increasing D_{A} does reduce the critical density.)

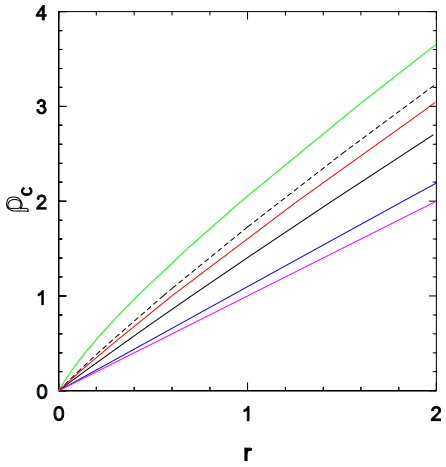

Figure 1. Mean-field predictions for the critical particle density ρ_c versus recovery rate r_c. Solid lines, top to bottom: $D_A = D_B = 0.2$; $D_A = 0.2$, $D_B = 1$; $D_A = 1$, $D_B = 1$; $D_A = D_B = 5$; rate equation result, $\rho_c = r$. Bold dashed line: two-site mean-field theory for the case $D_A = 1$, $D_B = 1$.

A richer description is obtained when we extend the approximation to two sites. There are (in general) 16 transitions into (and out of) a given state $(a, b; a', b')$. Using the symmetry $P(a, b; a', b') = P(a', b'; a, b)$, and factoring three-site probabilities so that $P(a, b; a', b'; a'', b'') = P(a, b; a', b')P(a', b'; a'', b'')/P(a', b')$, the equation governing the two-site joint probability can be written as

$$\begin{aligned}
\frac{\mathrm{d}P(a,b;a',b')}{\mathrm{d}t} &= \frac{D_A}{2}[(a+1)P(a+1,b;a',b') + (a'+1)P(a,b;a'+1,b') \\
&+ (a'+1)P(a-1,b;a'+1,b') + (a+1)P(a+1,b;a'-1,b')] \\
&\times \frac{D_B}{2}[(b+1)P(a,b+1;a',b') + (b'+1)P(a,b;a',b'+1) \\
&+ (b'+1)P(a,b-1;a',b'+1) + (b+1)P(a,b+1;a',b'-1)] \\
&+ \frac{D_A}{2}\left[\Phi_A(a-1,b)P(a-1,b;a',b') + \Phi_A(a'-1,b')P(a,b;a'-1,b')\right] \\
&+ \frac{D_B}{2}\left[\Phi_B(a,b-1)P(a,b-1;a',b') + \Phi_B(a',b'-1)P(a,b;a',b'-1)\right] \\
&+ r[(b+1)P(a-1,b+1;a',b') + (b'+1)P(a,b;a'-1,b'+1)] \\
&+ (a+1)(b-1)P(a+1,b-1;a',b') \\
&+ (a'+1)(b'-1)P(a,b,a'+1,b'-1) \\
&- \left\{D_A(a+a') + D_B(b+b') + \frac{D_A}{2}[\Phi_A(a,b) + \Phi_A(a',b')]\right. \\
&\left. + \frac{D_B}{2}[\Phi_B(a,b) + \Phi_B(a',b')] + r(b+b') + ab + a'b'\right\}P(a,b;a',b') \qquad (6)
\end{aligned}$$

where

$$\Phi_A(a,b) = \frac{\sum_{a'}\sum_{b'} a'\,P(a,b,a',b')}{P(a,b)} \qquad (7)$$

Table 1. Critical recovery rate r_c in one- and two-site mean-field approximations, compared with simulation.

D_A	D_B	r_c (1-site)	r_c (2-site)	r_c (sim)
0.5	0.25	0.5420	0.411	0.2325(10)
0.5	0.5	0.5771	0.429	0.1921(5)
0.25	0.5	0.5144	0.368	0.1585(3)

is the conditional A-particle density at a site, given that one of its nearest neighbours has occupancy (a, b). (Φ_B is defined analogously.) The above equations are integrated numerically using the fourth-order Runge–Kutta method and a cutoff of 10 for the variables a, b, a' and b'. For densities $\rho \leqslant 2$, the error incurred is negligible. Figure 1 shows that the two-site approximation predicts a larger value of ρ_c than does the one-site approximation, other parameters being equal.

We compare the mean-field predictions for the critical recovery rate against simulation for three representative cases (all for density $\rho = 1$) in table 1. The site approximation overestimates r_c by a factor of up to 3.3; in each case the two-site approximation yields a substantial improvement, although it still overestimates the critical value by a factor of up to 2.3. In principle, further improvement could be furnished using higher-order approximations, but in the present case the computational demands seem excessive. (The number of equations to be integrated in the n-site approximation is $[(a_c + 1)(b_c + 1)]^n$.)

An important aspect of the model is the anti-correlation between variables a and b at a given site. To quantify this we study

$$Q_A \equiv \frac{\langle ab \rangle}{\rho_B} - \rho_A = \frac{\mathrm{cov}(a, b)}{\rho_B}. \tag{8}$$

At the critical point ($\rho_B \to 0$), Q_A represents the excess density of A particles at a site bearing a B particle. In the one-site approximation we find (at the respective critical points) $Q_A = -0.583$, -0.298, and -0.0895, for $D_A = D_B = 0.2$, 1, and 5, respectively. That is, the species are anti-correlated, and the magnitude of the correlation decreases with increasing diffusion rate, as expected. This effect appears even more markedly in the two-site approximation, where, for example, $Q_A = -0.447$ at the critical point with $D_A = D_B = 1$. (All results quoted are for density $\rho = 1$.) Similar values are found in simulations. The two-site approximation shows that the anti-correlation of the numbers of A and B particles extends to the nearest neighbour site: $\langle a_j b_{j+1} \rangle / \rho_B - \rho_A = -0.444$ for the parameters noted above. The variables b_j and b_{j+1}, on the other hand, show a strong positive correlation.

Since diffusion of B particles is essential to the survival of the process, one might suppose that as D_B is reduced, the critical density would increase (for fixed recovery rate r), or the critical recovery rate r_c decrease (for fixed density). Mean-field theory (at both levels) predicts otherwise, as shown in figure 2: the critical recovery rate exhibits a minimum at a small value, D_B^*, of the B diffusion rate, but for even smaller values it grows rapidly. For $D_B > D^*$ the critical recovery rate grows systematically, and appears to saturate at the rate-equation value, $r_c = \rho$. Figure 2 shows that r_c follows the same qualitative trends in simulations as in the mean-field approximations, although its numerical value is (generally) considerably smaller.

The reason for the increase in r_c at small values of D_B appears to lie in the possibility of accumulating many B particles at a single site. Suppose that, by some fluctuation, a site acquires several B particles. Since $D_B \ll D_A$, this accumulation is relatively long-lived, and any A particles at this site will rapidly change to B, since the effective rate for the reaction $A \to B$, at this site, is b, which is large compared to r, the rate of the inverse reaction, and

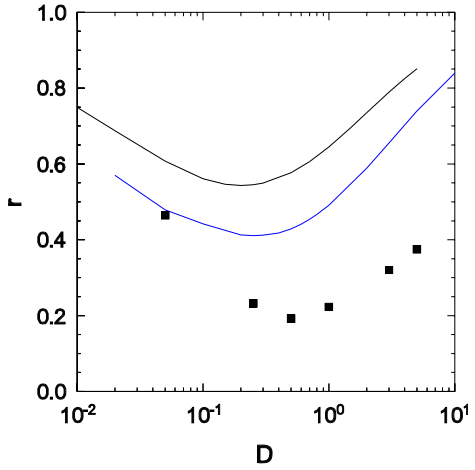

Figure 2. Critical recovery rate r_c versus B particle diffusion rate D_B, for $D_A = 0.5$ and $\rho = 1$. Upper curve: one-site MFT; lower curve: two-site MFT; points: simulation.

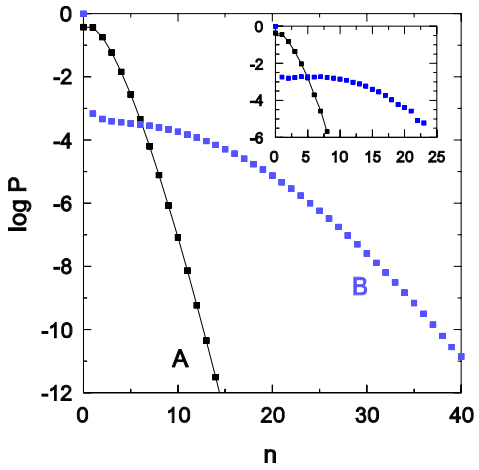

Figure 3. One-site probability distributions for the number of A and B particles. Main graph: one-site MFT, $\rho = 1$, $r \simeq r_c = 0.688$, $D_A = 0.5$ and $D_B = 0.02$. Inset: simulation result for $r = 0.5$ and the same values of ρ, D_A and D_B, system size $L = 500$.

also large compared to D_A. (Note as well that A particles straying onto such a site will readily change to B, and tend to remain at this site for a long time.) Indeed, for $D_B < D^*$, mean-field theory reveals that the one-site marginal distribution $P(b)$, though quite small for $b \geqslant 1$, decays very slowly with increasing b. The distributions $P(a)$ and $P(b)$ are compared in figure 3 (for the case $\rho = 1$, $r \simeq r_c = 0.688$, $D_A = 0.5$ and $D_B = 0.02$). Although (globally) almost all particles belong to species A, $P(b)$ decays much more slowly than $P(a)$ for large occupancies. (In this regime we increase a_c and b_c to 40 in the one-site MF calculations, to ensure that the cutoff does not affect the result.) $P(a)$ is well approximated by a Poisson distribution, while $P(b)$ shows strong deviations from this form. As shown in figure 3 (inset), similar distributions are observed in simulation, in the regime $D_B \ll D_A$.

4. Simulations

We perform Monte Carlo simulations using a simulation algorithm designed to reproduce faithfully the transition rates defining the process. Simpler, more efficient computational models involving the four types of transition (A and B diffusion, recovery (R) and infection (I)), are possible, but do not correspond to the same set of transition rates. Our simulation method permits quantitative comparison with theoretical predictions, including systematic expansions of the master equation [14].

The simulation consists of a sequence of events, each of which involves choosing the type of transition and the site at which it occurs. The choice of event type depends the total transition rates for each of the four processes, given by:

- Hopping of A particles: total transition rate $W_{\rm A} = N_{\rm A} D_{\rm A}$, where $N_{\rm A} = \sum_j a_j$ is the total number of A particles.
- Hopping of B particles: total transition rate $W_{\rm B} = N_{\rm B} D_{\rm B}$.
- Transformation of B particles to A particles: total transition rate $W_{\rm R} = r N_{\rm B}$.
- Transformation of A particles to B particles: total transition rate $W_{\rm I} = \sum_j a_j b_j$.

If we let $W_{\rm T} = W_{\rm A} + W_{\rm B} + W_{\rm R} + W_{\rm I}$ denote the total transition rate for all processes, then the probability that the next event is of type m (= A, B, R or I) is $P_{\rm m} = W_{\rm m}/W_{\rm T}$, while the mean time to the next event is $\Delta t = 1/W_{\rm T}$. (After each event the time is advanced by this amount.) The next event is chosen at random from this set of probabilities. Once the event type is determined, the site at which it occurs must be chosen. For this purpose a number of lists are maintained. For example, if the chosen event is hopping of an A particle, we select a site at random from a list of all sites (call it the A-list) having $a_j > 0$. Not all sites on the A-list, however, are equally likely to host the event: since each A particle has the same hopping rate, the probability of the event occurring at site j is proportional to a_j. We therefore keep track of the number $a_{\rm max}$ of A particles at the site with the largest number of such particles. When site j is chosen from the A-list, it is accepted for the next event with probability $p_{\rm acc} = a_j/a_{\rm max}$. In case of rejection, we again select a site (k, say) from the A-list and compare a_k with $a_{\rm max}$. In this manner we ensure that each A particle has the same likelihood of hopping. In a diffusion event the target site is chosen at random from the nearest neighbours of the original site.

The same procedure is adopted for the other three processes, necessitating the maintenance of a B-list and an AB-list (the latter containing all sites such that $a_j b_j > 0$). The rejection procedure outlined above, while necessary to maintain fidelity to the original transition rates, is computationally expensive. For this reason we restrict the present study to a relatively low density, $\rho = 1$, since in this case the maximum values, $a_{\rm max}$, $b_{\rm max}$ and $(ab)_{\rm max}$ are generally not very large. (One could in fact use lists of the positions of all A and B *particles*, instead of A- and B-bearing sites. But since the A–B reaction step requires an AB site list, we adopt a uniform procedure for all processes. Using particle lists instead of site lists for all processes except the A–B reaction could improve efficiency, particularly for large diffusion rates.)

In the studies reported here we sample the *quasi-stationary* (QS) distribution of the process, (that is, conditioned on survival), an approach that has been found to be very useful in the study of systems with an absorbing state [15]. (In fact, conventional simulations of 'stationary' properties of models with an absorbing state actually study the quasi-stationary regime, given that the only true stationary state for a finite system is the absorbing one.) We employ a recently devised simulation method that yields quasi-stationary properties directly [16]. This is done by maintaining, and gradually updating, a set of configurations visited during the evolution; when a transition to the absorbing state is imminent the system is instead placed in one of the saved configurations. Otherwise the evolution is identical to that of

a conventional simulation. (The set of saved configurations is updated by replacing one of the saved configurations with the current one, with a small probability $p_{\rm rep}$ at each time step.)

The above scheme was shown [16] to yield precise results, in accord with the exact QS distribution for the contact process on a complete graph, and with conventional simulations of the same model on a ring [16]. The scheme has also been shown to yield results that agree, to within uncertainty, with the corresponding results of conventional simulations for a sandpile model [17]. The advantage of the method is that a realization of the process can be run to arbitrarily long times. Thus, whereas in conventional simulations a large number of realizations must be performed to have a decent sampling of the quasi-stationary state, here every realization provides useful information. This leads to an order of magnitude improvement in efficiency in the critical region. The application of the QS simulation method to discontinuous transitions is discussed in section 5 below. For further details on the method see [16].

We performed extensive simulations of the DEP on rings of $L = 200$, 500, 1000, 2000 and 4000 sites, using the QS method. The number of saved configurations M ranges from 1000, for $L = 200$, to 100 for $L = 4000$. Values of $p_{\rm rep}$ range from 10^{-4} to 10^{-5} (smaller values for larger systems). Two time scales appear to be relevant in the choice of the replacement probability $p_{\rm rep}$. One is the mean residence time of a configuration on the list, $\tau_L = M/p_{\rm rep}$. The other is the QS lifetime τ, i.e. the mean time between attempts to visit the absorbing state. We find that our results are independent of the choice of $p_{\rm rep}$ provided that $\tau/\tau_L < 1$. This appears to be associated with the need to preserve configurations visited prior to the last attempted transition to the absorbing state. Of course one could make τ_L arbitrarily large by reducing $p_{\rm rep}$, but this would prolong the memory of the initial state. (For this reason, we use a $p_{\rm rep}$ ten times larger during the relaxation phase. The latter represents about 10% of the total simulation time.)

Initially, half the particles are of type A and half of type B; the particles are distributed randomly and independently over the sites, so that the distribution of a and b at a given site is essentially Poisson with mean 1/2. Each realization of the process runs for a certain maximum time, $T_{\rm m}$, of up to 10^8 time units. The results reported here represent averages over 4–12 independent realizations for each set of parameter values. Averages are taken in the QS regime, after discarding an initial transient, with a duration that depends on the system size. In practice we accumulate histograms of the time during which the system has exactly $1, 2, \ldots n, \ldots,$ B particles. The histograms are used to evaluate the mean B particle density, $\rho_{\rm B}$, and the moment ratio [18]

$$m = \frac{\langle b^2 \rangle}{\langle b \rangle^2}. \tag{9}$$

We determine the critical recovery rate $r_{\rm c}(\rho, D_{\rm A}, D_{\rm B})$ using the criteria of power-law dependence of $\rho_{\rm B}$ and τ on system size L (i.e. the usual finite-size scaling relations $\rho_{\rm B} \sim L^{-\beta/\nu_\perp}$ and $\tau \sim L^z$). To probe the three characteristic regimes of the process, three cases are studied in detail: $D_{\rm A} = D_{\rm B} = 0.5$; $D_{\rm A} = 0.5$, $D_{\rm B} = 0.25$; and $D_{\rm A} = 0.25$, $D_{\rm B} = 0.5$.

Consider first the case $D_{\rm A} = 0.5$, $D_{\rm B} = 0.25$. Since it has been suggested that the phase transition is discontinuous for $D_{\rm A} > D_{\rm B}$, it is of interest to study the behaviour of the order parameter $\rho_{\rm B}$ as a function of the recovery rate r. In figure 4 we plot estimates for the order parameter in the limit $L \to \infty$, based on our data for $L = 200$–4000. (The extrapolation can only be performed reliably for $r \leqslant 0.22$ with the data at hand.) It appears that the order parameter decays *continuously* to zero as $r \to r_{\rm c} \simeq 0.23$. We cannot rule out a weakly discontinuous transition on the basis of these data, but a continuous transition seems the more natural interpretation. The evidence for a continuous transition is greatly strengthened by our observation of critical scaling, as we now discuss.

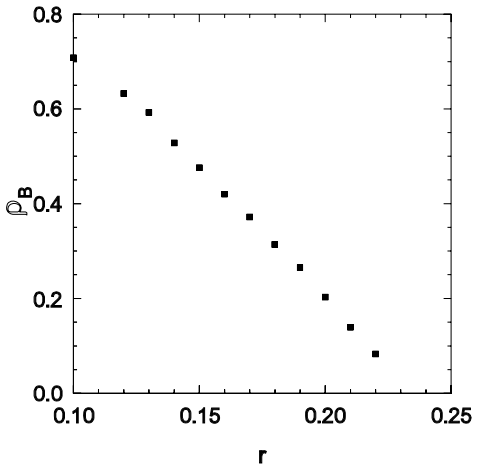

Figure 4. Order parameter ρ_B versus recovery rate for $D_A = 0.5$, $D_B = 0.25$ and $\rho = 1$. The points represent extrapolations to the infinite-size limit based on data for sizes $L = 200$–4000.

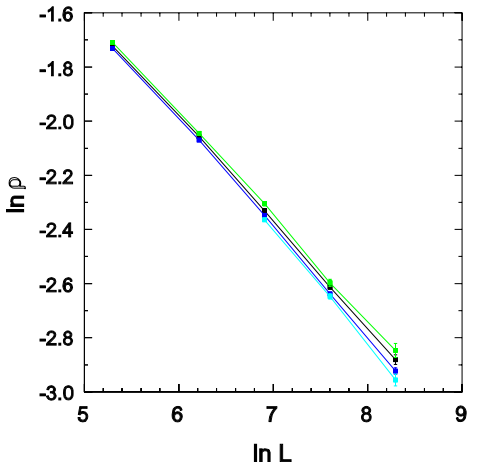

Figure 5. Order parameter ρ_B versus system size L, for the same parameters as figure 4. From top to bottom: recovery rate $r = 0.231, 0.232, 0.233, 0.234$.

Data for the QS order parameter ρ_B versus system size L are shown on log scales (for the case $D_A = 0.5$, $D_B = 0.25$) in figure 5. The data for $r = 0.231$ curve upward, while those for $r = 0.234$ curve downward, leading to the estimate $r_c = 0.2325(10)$. For this range of values we see good evidence of power-law scaling, as expected at a critical point. Similarly, the data for the QS lifetime τ (see figure 6) show power-law scaling for $r \simeq r_c$, and significant curvature away from r_c.

As a check on our procedure for determining r_c, we also perform, for $D_A = 0.5$, $D_B = 0.25$, initial decay studies [19, 20]. In these studies the order parameter ρ_B is followed as a function of time, using the same initial condition as in the QS studies. (Due to the large system size, the process does not enter the absorbing state on the time scale of the simulation.) Here the expected critical behaviour is $\rho_B \sim t^{-\theta}$. Using deviations from the power law to identify off-critical values, a study of systems of 10^6 sites, to a maximum time of 10^7, enables

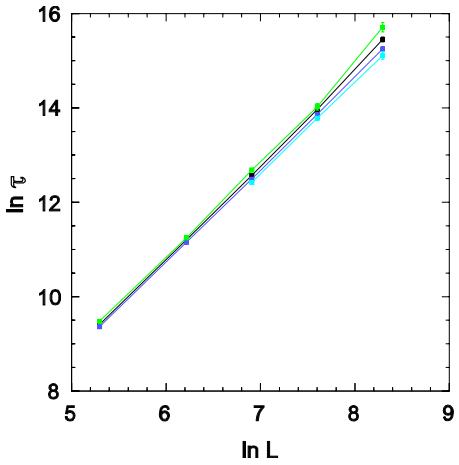

Figure 6. Lifetime τ versus system size L, symbols and parameters as in figure 5.

Table 2. Critical parameters from simulation.

D_A	D_B	$\beta/\nu_\perp$	z	$\nu_\perp$	m
0.5	0.25	0.404(10)	2.01(4)	2.3(3)	<1.15
0.5	0.5	0.192(4)	2.02(4)	2.0(2)	1.093(10)
0.25	0.5	0.113(8)	1.6(2)	1.77(3)	1.06(1)

us to restrict r_c to the interval [0.231, 0.239]. This is consistent with, but less precise than, the QS results. Analysis of the data for $t \geqslant 5 \times 10^5$ furnishes $\theta \simeq 0.5$. The lack of precision in these studies and in our result for the moment ratio highlights the slow convergence of these simulations, presumably reflecting strong finite-size effects.

The studies described above lead to estimates for the critical exponent ratios $\beta/\nu_\perp$ and $z = \nu_\parallel/\nu_\perp$. To obtain a direct estimate of $\nu_\perp$, we study the order parameter in the neighbourhood of the critical point r_c for various lattice sizes. This permits us to estimate the correlation length exponent $\nu_\perp$, using the finite-size scaling relation for the order parameter,

$$\rho_B(\Delta, L) \propto L^{-\beta/\nu_\perp} \mathcal{F}(L^{1/\nu_\perp}\Delta), \tag{10}$$

where $\Delta = r - r_c$ and $\mathcal{F}$ is a scaling function. This implies

$$\left|\frac{\partial \ln \rho_B}{\partial r}\right|_{r_c} \propto L^{1/\nu_\perp}. \tag{11}$$

For the case $D_A = 0.5$, $D_B = 0.25$, the data for $L = 500$, 1000, 2000 and 4000 yield the estimate $\nu_\perp = 2.3(3)$. We performed similar finite-size scaling analyses for the other cases.

The moment ratio m is also useful in characterizing critical behaviour. Our results, shown in figure 7, lead to estimates for the limiting ($L \to \infty$) value except in the case $D_A = 0.5$, $D_B = 0.25$, for which the moment ratio decreases systematically with system size L. The trend to smaller values of m with increasing D_B/D_A may reflect the reduced tendency for B particles to accumulate at a given site. Our results for the critical parameters are summarized in table 2.

Some insight into the distinctive behaviours for $D_A > D_B$ and $D_A < D_B$ is afforded by plots of the space–time evolution of the process. Figure 8 presents a typical sequence of density profiles for $D_A = 0.5$ and $D_B = 0.25$ in a system of 4000 sites, with $r = 0.22$. The black lines represent the local density of B particles (averaged in blocks of 50 sites) and the lighter lines

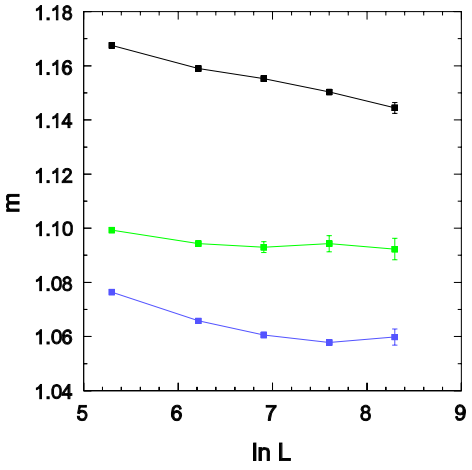

Figure 7. Moment ratio m versus system size L, at the critical point r_c, for (upper to lower) $D_A = 0.5$, $D_B = 0.25$; $D_A = D_B = 0.5$; and $D_A = 0.25$, $D_B = 0.5$.

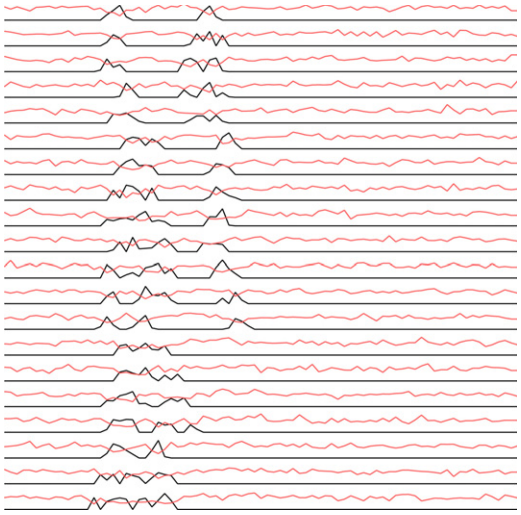

Figure 8. Space–time evolution of the DEP as described in text, for $D_A = 0.5$, $D_B = 0.25$.

that of A particles. Each scan is separated by an interval of $\Delta t = 50\,000$ time units, with time increasing downward. Of note is the very slow evolution of the regions with $\rho_B > 0$, which are quite sparse. The reduction in ρ_A in these regions is also evident. A similar plot, but for $D_A = 0.25$, $D_B = 0.5$ and $r = 0.16$ and using $\Delta t = 10\,000$, is shown in figure 9. Here the B density is more uniform, and evolves more rapidly.

We close this section with the observation that the DEP is characterized by unusually large and long-lived fluctuations, which make it difficult to obtain precise results in simulations. In the case of the contact process, for example, a system size of $L = 1000$ is sufficient for the determination of critical exponents to rather high precision. As in other models dominated by diffusion, such as conserved sandpiles [17] and the diffusive pair contact process (PCPD) [21, 22], scaling properties of the DEP emerge clearly only at larger sizes. One signal of this is the slow convergence (with L) of the order parameter moment ratio m.

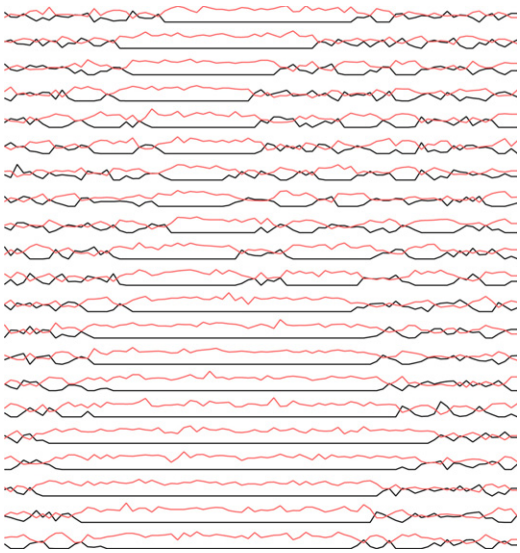

Figure 9. Space–time evolution of the DEP as in figure 7, but for $D_A = 0.25$, $D_B = 0.5$.

5. Quasi-stationary simulations at a discontinuous phase transition

As shown in [15, 23], the quasi-stationary probability distribution is bimodal in the vicinity of a discontinuous phase transition to an absorbing state. The latter studies, however, involve mean-field-like approximations, so the conclusions cannot be extended directly to lattice models with spatial structure. A key issue is whether the QS simulation method can be used to identify discontinuous transitions, or whether the simulation becomes trapped in one of the metastable branches, which could yield an apparently continuous transition even in the case of a truly discontinuous one.

To analyse this question we apply the QS simulation method to the one-dimensional triplet creation model (TCM) [24], in which a particle (X) undergoes diffusion, annihilation ($X \to 0$) and catalytic creation ($3X \to 4X$), with probabilities D, $(1 - D)/(1 + \lambda)$ and $\lambda(1 - D)/(1 + \lambda)$, respectively. (In this model each site may be occupied by at most one particle; creation depends on the occupation of three successive sites.) In [24] the transition between the active and absorbing states was found to be continuous for smaller diffusion probabilities, but discontinuous for $D \geqslant 0.9$. The existence of discontinuous transitions in one-dimensional systems was questioned in [25], but recent studies using the conservative version of the process, and critical spreading simulations [26, 27] have vindicated the findings of [24].

We studied the TCM with diffusion probability $D = 0.95$ on rings of 2000, 5000, 10 000 and 20 000 sites. Figure 10 shows the order parameter ρ (the particle density) as a function of the creation parameter λ. Despite finite-size rounding, the data clearly suggest a discontinuity in $\rho(\lambda)$ near the point $\lambda = 10.11$. A typical example of the space–time evolution of the TCM near the phase transition point is shown in figure 11. Of note is the generally high particle density in the active regions. This impression is quantified in the cell-occupancy histogram (figure 12, for cells of 50 sites), showing a distinctly bimodal distribution. The coexistence of high-density active regions with inactive ones is again consistent with a discontinuous phase transition.

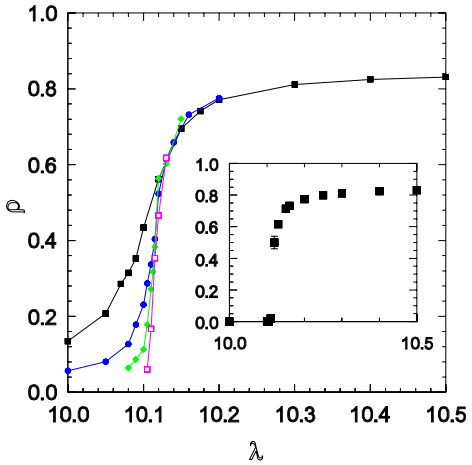

Figure 10. Particle density ρ versus creation parameter λ in the triplet creation model with $D = 0.95$ Main graph: results for system sizes $L = 2000$, 5000, 10 000 and 20 000 (in order of increasing steepness). Inset: extrapolation to infinite size.

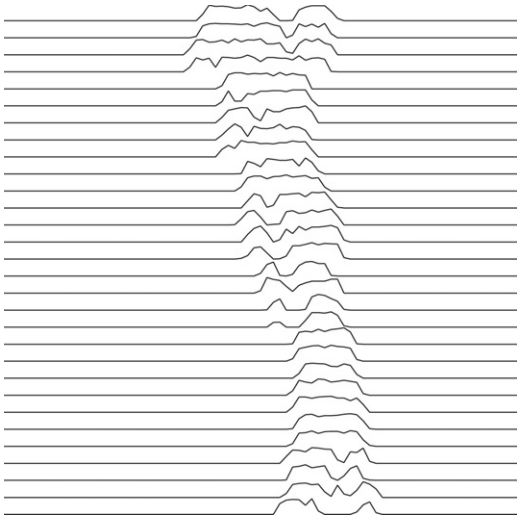

Figure 11. Space–time evolution in the triplet creation model with $D = 0.95$, $\lambda = 10.10$, and system size $L = 4000$, time interval $\Delta t = 10\,000$.

We find even stronger evidence of a discontinuous phase transition in the *asymmetric* triplet creation model (ACTM), in which particles may only hop in one direction. QS simulations reveal two distinct branches of the order parameter for $D = 0.9$. In the region where the two branches coexist, the order parameter histogram is bimodal. The time series for the order parameter exhibits sudden jumps between high- and low-density regimes.

Our results for the TCM and ACTM show that the quasi-stationary simulation method is useful in identifying discontinuous phase transitions. These results may be contrasted with those for the DEP with $D_A > D_B$. In the latter case there is no suggestion of a discontinuity in $\rho(r)$, and the local occupancy histogram shows no evidence of coexisting phases.

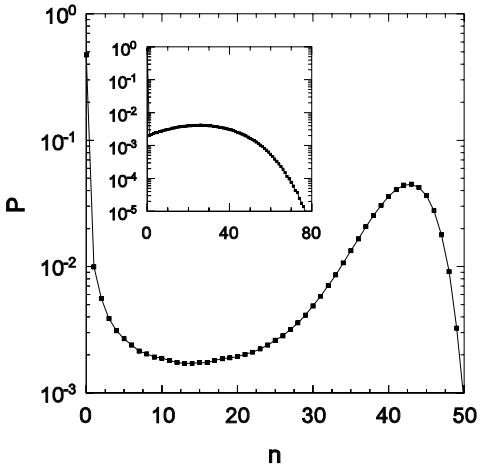

Figure 12. Main graph: cell-occupancy histogram in the TCM, for the same parameters as figure 10. Inset: cell-occupancy histogram for the DEP with $D_A = 0.5$, $D_B = 0.25$, $r = 0.233$, and $L = 4000$.

6. Discussion

We studied the one-dimensional diffusive epidemic process using mean-field approximations and Monte Carlo simulations. Mean-field theory provides a qualitative description of the phase diagram, and reveals a surprising, nonmonotonic dependence of the critical recovery rate on the B particle diffusion rate, confirmed in simulation. This reflects the tendency (for $D_B \ll D_A$) for many B particles to accumulate at a single site, as revealed the one-site probability distribution $P(b)$. Mean-field theory also captures qualitatively the anti-correlation in the number of A and B particles at a single site.

Although our simulations do not extend to sufficiently large systems to furnish precise values of critical exponents, our results, especially for the ratio $\beta/\nu_\perp$, clearly support the scenario of distinct universality classes for the three cases, $D_A < D_B$, $D_A = D_B$ and $D_A > D_B$. The transition in the one-dimensional system appears to be continuous in all cases, as already observed in [9].

The question of discontinuous absorbing-state phase transitions in one-dimensional nonequilibrium systems has been a subject of some controversy [24–27]. The existence of such a transition in the triplet creation model now seems well established, and is consistent with our QS simulations of the model and of its anisotropic version. While a discontinuous transition in the one-dimensional DEP is not, therefore, ruled out in principle, we find no evidence for such a transition. It is perhaps worth mentioning that the present results do not completely exclude the possibility of a weakly discontinuous transition in the DEP.

The diffusive epidemic process features a conserved total particle density, as does the conserved stochastic sandpile and conserved lattice gas, models that are believed to belong to the same universality class (see [17] and references therein). In the sandpile, isolated particles are inactive; an inactive particle is activated (and is able to diffuse) when an active particle hops onto its site. This suggests that inactive and active particles in the sandpile be identified with A and B particles in the DEP. On this view, the essential difference between the sandpile and the DEP is that in the former, inactive particles do not hop at all, rendering the sandpile the $D_A \to 0$ limit of the DEP. It is natural to ask whether the stochastic sandpile falls in the

same universality class as the DEP with $D_A < D_B$. Comparing the critical exponent values for the one-dimensional sandpile, $\beta/\nu_\perp = 0.21(1)$, $z = 1.50(4)$ and $\nu_\perp = 1.35(2)$, with the corresponding values for the DEP (table 2), one is led to the conclusion that the two models belong to distinct classes. It is possible, however, that the DEP with $D_A = 0$ belongs to the conserved sandpile universality class, a question we defer to future studies.

Renormalization group analysis [1, 8, 10, 12] predicts (independent of the relative magnitudes of D_A and D_B) that $z = 2$ and $\nu_\perp = 2/d$. The simulation results are consistent with these predictions *except* for the case $D_A = 0.25$, $D_B = 0.5$, for which our estimates are significantly smaller. This may be due to the slow convergence noted above. We hope to address this point in future studies of larger systems. It would also be of interest to verify that the critical exponents are in fact insensitive to changes in the diffusion rates, within the three universality regimes that have been established. We expect the present results to serve as a point of reference for studies based on systematic expansions of the master equation.

Acknowledgments

We are grateful to Hugues Chaté for helpful comments. This work was supported by CNPq and Fapemig, Brazil.

References

[1] Kree R, Schaub B and Schmittmann B 1989 *Phys. Rev.* A **39** 2214
[2] Marro J and Dickman R 1999 *Nonequilibrium Phase Transitions in Lattice Models* (Cambridge: Cambridge University Press)
[3] Hinrichsen H 2000 *Adv. Phys.* **49** 815
[4] Lübeck S 2004 *Int. J. Mod. Phys.* B **18** 3977
[5] Ódor G 2004 *Rev. Mod. Phys.* **76** 663
[6] Jensen I 1993 *Phys. Rev. Lett.* **70** 1465
[7] Jensen I and Dickman R 1993 *J. Phys. A: Math. Gen.* **26** L151
[8] Oerding K, van Wijland F, Leroy J P and Hilhorst H J 2000 *J. Stat. Phys.* **99** 1365
[9] Fulco U L, Messias D N and Lyra M L 2001 *Physica* A **295** 49
Fulco U L, Messias D N and Lyra M L 2001 *Phys. Rev.* E **63** 066118
[10] van Wijland F, Oerding K and Hilhorst H J 1998 *Physica* A **251** 179
[11] de Freitas J E, Lucena L S, da Silva L R and Hilhorst H J 2000 *Phys. Rev.* E **61** 6330
[12] Janssen H-K 2001 *Phys. Rev.* E **64** 058101
[13] de Freitas J E, Lucena L S, da Silva L R and Hilhorst H J 2001 *Phys. Rev.* E **64** 058102
[14] Maia D S and Dickman R 2006 unpublished
[15] Dickman R and Vidigal R 2002 *J. Phys. A: Math. Gen.* **35** 1147
[16] de Oliveira M M and Dickman R 2005 *Phys. Rev.* E 016129
[17] Dickman R 2006 *Phys. Rev.* E **73** 036131
[18] Dickman R and Leal da Silva J K 1998 *Phys. Rev.* E **58** 4266
[19] Kockelkoren J and Chaté H 2003 *Phys. Rev. Lett.* **90** 125701
[20] Park S-C and Park H 2006 *Phys. Rev.* E **73** 025105(R)
[21] Henkel M and Hinrichsen H 2004 *J. Phys. A: Math. Gen.* **37** R117
[22] de Oliveira M M and Dickman R 2006 *Phys. Rev.* E **74** 011124
[23] de Oliveira M M and Dickman R 2004 *Physica* A **343** 525
[24] Dickman R and Tomé T 1991 *Phys. Rev.* A **44** 4833
[25] Hinrichsen H 2006 *Preprint* cond-mat/0006212
[26] Fiore C E and de Oliveira M J 2004 *Phys. Rev.* E **70** 046131
[27] Cardozo G O and Fontanari J F 2006 *Eur. J. Phys.* B **51** 555